P. KURTYKA*, I. SULIMA*[#], P. HYJEK**, L. JAWORSKA**

INFLUENCE OF HIGH PRESSURE-HIGH TEMPERATURE METHOD ON THE SELECTED MECHANICAL PROPERTIES OF STEEL AISI 316L WITH 2% TiB$_2$

AISI 316L/TiB$_2$/2p composites were manufactured by HP-HT using different pressures (5 and 7 GPa) and temperatures (900-1300°C), with constant reinforcing particle content 2 vol%. The mechanical properties of the composites were evaluated on the basis of hardness (HV0.3) and compression tests (20°C, 10^{-5} s^{-1}). The results showed that the role of sintering pressure increased with increasing process temperature. At temperatures of 900°C and pressures of 5 and 7 GPa the difference in measured values of compressive strength was 1-2%, while at 1300°C they reached 20%. At constant pressure of 5 GPa, a change in hardness and compressive strength of 40% were obtained with a temperature change of 900 to 1300°C. Changes in mechanical properties in the composite occurred without substantial changes in density, microstructure, reinforcement phase distribution, and phase composition in the matrix.

Keywords: High Pressure-High Temperature, Physical Properties, Mechanical Properties, Steel Matrix Composites, Titanium Diboride

1. Introduction

In the area of materials engineering, research works are undertaken on the development of advanced materials, with attention focused on special opportunities to develop new manufacturing technologies for these materials. One of the most promising groups of advanced materials is the metals reinforced by ceramic particles. The developments in this group of materials are characterized not only by the invention of new manufacturing technologies, but also and mainly by the achievement of better physical and chemical properties. Currently, titanium diboride is a material with a growing interest among various ceramics, due to its unique physical, chemical and mechanical properties [1-3]. In contrast, iron base alloys are used as the matrix of metal composite materials, because of their low cost, good mechanical properties and wear resistance [4,5].These materials allow for a significant reduction in cost compared to existing competing materials. High interest composite steel (steel-matrix composites) are associated with obtaining high strength, modulus and wear, corrosion resistance than could not be achieved for a conventional alloy [6-9]. Numerous studies, confirmed the importance of manufacturing methods (in situ or ex situ) and their influence on microstructures especially, on reinforcing phases (distribution, shape, size). Papers also shown the effects on the stress-strain curves, plastic flow, hardness, for this type of materials etc. Particularly interesting seem to be all the is-sues related to the impact of manufacturing process parameters, especially as regards the more advanced techniques like HP-HT (High Pressure-High Temperature) [10,11], FAST/SPS (Field Assisted Sintering Technique/Spark Plasma Sintering) [12], SHSB (Self Propagating High Temperature Synthesis in Bath) [13-16], ECAP (Equal-channel angular pressing) or KoBo [12,17-20], FSP (Friction Stir Processing) [21-23], on changes in hardness, the waveforms of related curves, and other mechanical properties. The paper presents the results of studies regard to influence of manufacturing process parameters on the physical properties, hardness, plastic flow and shape of the stress-strain curves of the AISI 316L/TiB$_2$/2p composite. The key differences in selected properties of the examined composite have been presented in correlation with the parameters of the HP-HT process. Investigations have been made to answer the question what impact the high pressure and temperature may have on selected properties of the composite material.

1.1. High Pressure-High Temperature technology

High pressure sintering process is one of the techniques which restrain the growth and accelerate the densification process. The important advantage of the HP-HT sintering method is the possibility of simultaneous exposure to high pressure and high temperature. The consequence of the simultaneous

*   PEDAGOGICAL UNIVERSITY OF KRAKOW, INSTITUTE OF TECHNOLOGY, 2 PODCHORAZYCH STR., 30-084, KRAKOW, POLAND
** AGH UNIVERSITY OF SCIENCE AND TECHNOLOGY, FACULTY OF NON-FERROUS METALS, AL. MICKIEWICZA 30, 30-059 KRAKÓW, POLAND

[#]   Corresponding author: iwona.sulima@up.krakow.pl

application of high pressure and high temperature is flexibility in reducing the time of the sintering process to tens of seconds, when the traditional methods usually last a few or several hours. The effect of sintering method using HP-HT is high degree of densification of the sintered product tending to 100% combined with the ability to obtain simultaneously a fine microstructure. HP-HT method is applied in the sintering process of a large group of materials, to mention diamond, regular boron nitride (cBN), TiB$_2$ ceramics, gradient materials, as well as intermetallics and composites [24-27]. Details of the process and its opportunities are more widely reported in the literature [28,29]. The HP-HT method was choice because very short duration of sintering process and pressure participation during this process.

2. Materials and experimental methods

2.1. Materials

The starting materials used in this study were commercial titanium diboride powder (Atlantic Equipment Engineers, 10 µm grade, purity 99.9%) and AISI 316L austenitic stainless steel powder (Hoganas, 45 µm grade). The chemical compositions of the AISI 316L steel powder and TiB$_2$ ceramic powder under study are given in Table 1 and Table 2.

TABLE 1

Chemical composition (wt %) of AISI 316L stainless steel powder, balanced Fe

C	Cr	Ni	Mo	Mn	Si	S	P
0.027	17.20	12.32	2.02	0.43	0.89	0.03	0.028

TABLE 2

Chemical composition (wt %) of TiB$_2$ powder

B	O	C	N	Fe	Ti
30.1	1.6	0.36	0.32	0.06	Bal.

2.2. Manufacturing process

The raw powders were prepared by milling in a planetary mill Pulverisette 6 Mono for 6h. The initial phase composition of mixtures for the sample preparation was 98 vol% AISI 316L + 2 vol% TiB$_2$. Next, the mixture of powders was formed into discs (diameter d – 15 mm, height h – 5 mm) by pressing in a steel matrix under the pressure of 200 MPa. The sintering process was carried out using a high pressure-high temperature (HP-HT) Bridgman type apparatus. Figure 1 presents a scheme of the chamber for high-pressure sintering with spherical anvils of the Bridgman type. The samples were sintered at temperatures of 900 °C, 1150°C and 1300°C and the pressures of 5 ± 0.2 GPa and 7 ± 0.2 GPa. The sintering parameters are given in Table 3 were determined on the basis of reports in the literature [31-33] and our own experience.
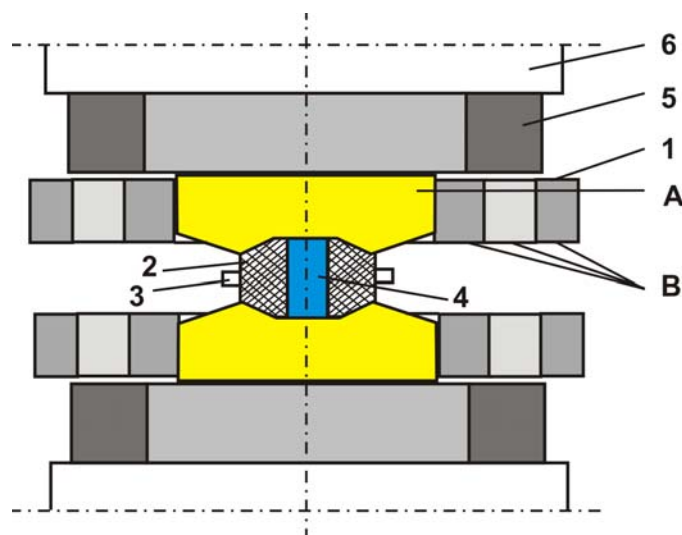

Fig. 1. Scheme of the chamber for high-pressure sintering with spherical anvils of the Bridgman type [30] where: 1 – anvil (A – central part made of sintered carbides, B – supporting steel rings), 2 – pyrophyllite container, 3 – pyrophyllite gasket, 4 – material for sintering, 5 – punch, 6 – supporting plate.

2.3. Measurements

The density was determined by weighing in air and water using the Archimedes method. The uncertainty of the measurements was 0.02 Mg/m^3. The Youngs modulus of the composites was measured based on the velocity of ultrasonic waves transition through the sample using a Panametrics Epoch III ultrasonic flaw detector. The velocities of the transverse and longitudinal waves were determined as the ratio of sample thickness and relevant transition time. The accuracy of the calculated Youngs modulus was estimated at 2%. Calculations were made using the following formula (1):

$$E = \rho C_T^2 \frac{3C_L^2 - 4C_T^2}{C_L^2 - C_T^2} \qquad (1)$$

where: E – Youngs modulus, C_L – longitudinal wave velocity, C_T – transversal wave velocity, ρ – material density.

TABLE 3

Sintering parameters, Wa – duration of the heating, St – sintering, Co – cooling

Sample	P [GPa]	T [°C]	Wa [s]	St [s]	Co [s]
S5-1	5	900	5	60	5
S5-2	5	1150	5	60	5
S5-3	5	1300	5	60	5
S7-1	7	900	5	60	5
S7-2	7	1150	5	60	5
S7-3	7	1300	5	60	5

The microstructure investigations were conducted using a JEOL JSM 6460 LV scanning electron microscope with secondary electron imaging (SEI) and backscattered electron imag-

ing (BEI) detection modes, Oxfords Energy Dispersive X-ray Spectroscopy (EDS) microprobe and Aztec Software.

For the analysis of phase composition, an X-ray Kristaloflex D500 diffractometer made by SIEMENS with Cu tube radiation (lambda = 0.154 nm) was used.

The Vickers hardness tests were made on an Innovatest 4303 hardness machine with a load of 3N and in accordance with the European standard EN ISO 6705-1.

The mechanical properties of the composites were also tested in the compression test on a modified version of the Instron TT-DM machine equipped with an electronic measuring circuit. Tests were performed on cylindrical samples with h to d ratio of 1.5, cut out from the sintered materials. Tests were performed at 20°C with an initial strain rate equal to 10^{-5} s $^{-1}$.

The analysis of hardening ranges was carried out according to the methodology proposed by Ludwigson [34] using the following formula (2):

$$\sigma = K_1 \varepsilon^{n_1} \pm e^{(K_2 + \varepsilon n_2)} \tag{2}$$

and methodology proposed by Hollomon [35] using the following formula (3):

$$\sigma = K_1 \varepsilon^{n_1} \tag{3}$$

where: σ and ε – the real stress and real strain respectively, $K_{1,2}$ – strength coefficients, $n_{1,2}$ – strain hardening exponent.

The K_1 and n_1 parameters are often used to assess the behaviour in both uniaxial compression and/or tension tests at room and at elevated temperatures [36-39].These constants have also been used to relate the tensile and compression properties to hardness behavior, metal forming and many other phenomena. Intensive researches are made to understand the physical significance of these parameters by correlation with the materials microstructures, grain size, yield strength etc. [40-44].

3. Research and Discussion

3.1. Physical properties

Studies of basic physical properties of the composites allowed determining the density and Young's modulus for sinters obtained under different conditions of pressure and temperature. It was observed that in the case of the manufactured AISI 316L/TiB$_2$/2p composites, the selected sintering conditions had no significant effect on its density. The values obtained were at a level between 7.77 Mg/m^3 (for the composite obtained at 900°C and a pressure of 7 GPa) and 7.83 Mg/m^3 (for the composite obtained at 1300°C and a pressure of 5 GPa), which corresponded to 99% of the theoretical density. The obtained results confirm the validity of the sintering process and proper selection of its parameters. The similar tendency is for in the case of Young's modulus. There was a mild, i.e. not exceeding a few percent, influence of sintering parameters on the obtained values of the modulus of elasticity. Young's modulus correlated with the sintering temperature and pressure is shown in Figure 2. The

accuracy of calculated Young's modulus is estimated at 2%. The maximum value of Young's modulus was obtained in the samples sintered at a pressure of 5 GPa and a temperature of 1300°C and it amounted to 95% of the theoretical value, while the lowest value was 91% and it was obtained in the samples sintered at temperatures of 900°C and 1150°C and a pressure of 7 GPa. The results show that both temperature and pressure within the accepted range of production parameters have no major effect on the density and Young's modulus of the tested composite.
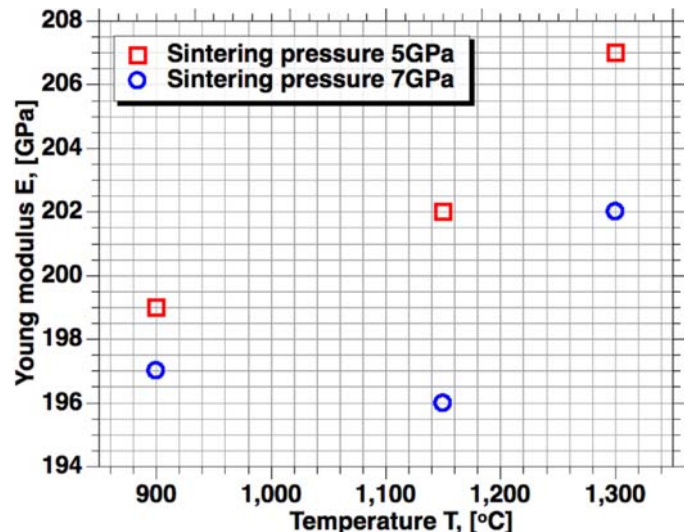

Fig. 2. The effect of temperature and pressure on the Young's modulus of the AISI 316L/TiB$_2$/2p composites fabricated by the HP-HT process

3.2. Mechanical properties

Similar analysis of the effect of manufacturing parameters on the mechanical properties was carried out using the results of hardness measurements and compression tests. The effect of sintering pressure and temperature on hardness of the AISI 316L/TiB$_2$/2p composite is shown in Figure 3. A minimum of six hardness measurements were made for each sample. Standard deviations of HV0.3 values were no more than 4% of the average values.

Regardless of the applied pressure and temperature of sintering, significant differences were observed in the hardness values. Figure 3 clearly shows the negative effect of high temperature of the manufacturing process on the value of the HV 0.3 hardness number.

For the pressure of 5 GPa, the observed decrease in hardness values amounted to about 40%, while for the pressure of 7 GPa it reached the level of about 30%. It should also be noted that for the samples produced at different sintering pressures of 5 GPa and 7 GPa but at the same temperature, the resulting hardness differences were of 15% at maximum. These results demonstrate a pronounced effect of temperature and much less pronounced effect of pressure on the composite hardness. For sintered AISI 316L steel without TiB$_2$ additive, the decrease in hardness values as a function of sintering temperature was about
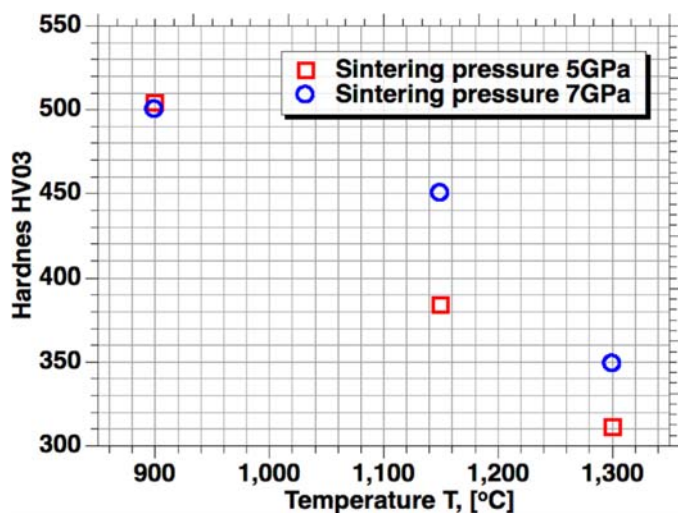
1588

Fig. 3. Changes in the hardness HV 0.3 related to the temperature and pressure parameters of the sintering process of the AISI 316L/TiB$_2$/2p composites

20%, independently of the applied sintering pressure. However, no significant effect of sintering pressure on the hardness of pure steel was observed.

However, given the fact that in the case of composite materials, hardness measurements may carry errors resulting, from e.g. differences in the distribution of the reinforcing phase [23,45], the results of compression tests were adopted as the representative ones and allowing the determination of macroscopic mechanical properties of the AISI 316L/TiB$_2$/2p composites.

The performed compression tests enabled evaluating the impact of sintering conditions on the parameters of equations describing the ranges of the AISI 316L/TiB$_2$/2p composite hardening. The mechanical deformation characteristics of composites studied in a true stress – true strain ($\sigma - \varepsilon$) system are shown in Figure 4.

As can be seen, the changing production parameters significantly affect the stress of the composite plastic flow and the run of $\sigma - \varepsilon$ curves. It has been found that, besides the sintering temperature, the values of the compressive strength obtained in individual samples are also dependent on pressure. The importance of this parameter is increasing with the increasing temperature of sintering. In the case of the sintering temperature of 900°C, the differences between the values of s for the pressure of 5 GPa and 7 GPa are only 1-2%, and in principle it can be assumed that they are comprised within the limits of measurement error. However, at a temperature of 1300°C, the differences in the compressive strength values reach almost 20%. A much stronger effect was observed in samples sintered at different temperatures but constant pressure. The maximum difference was reported for the sintering pressure of 5GPa, when the values of s for the temperatures of 900°C and 1300°C differed by almost 40%. For the pressure of 7GPa, the differences were much smaller and amounted to approximately 25%. For the AISI 316L austenitic steel, the differences between the values of Rc for the pressure of 5 GPa and 7 GPa, at a sintering temperature of 1000°C and 1300°C, are 8% and 13% respectively [9].
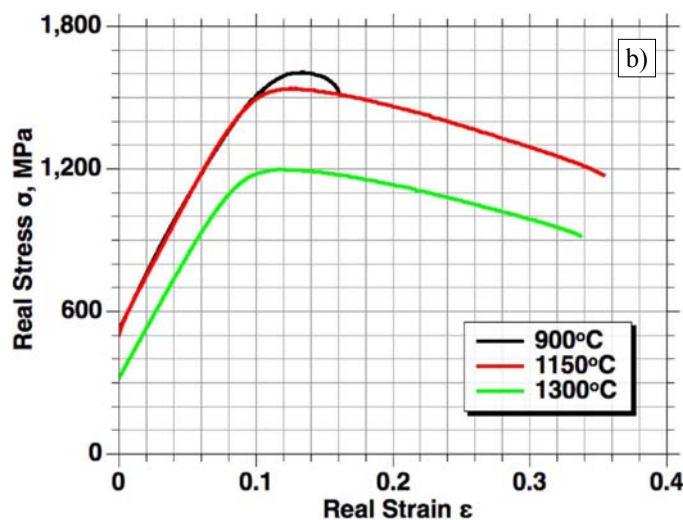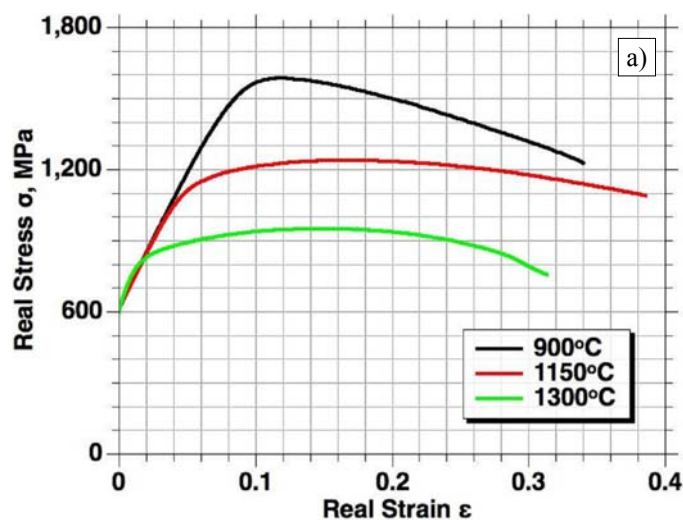

Fig. 4. Mechanical characteristics of the compression of samples after the HP-HT process conducted under conditions listed in Table 3: a) 5 GPa, b) 7 GPa
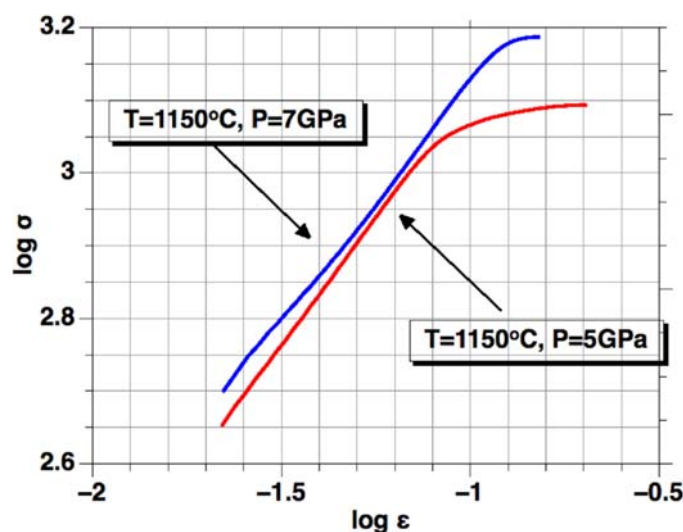

Fig. 5. Example of different types of the deformation curves plotted in a log(σ) − log(ε) system for the two extreme cases of the S5-2 (5 GPa, 1150°C) and S7-2 (7 GPa, 1150°C) composites
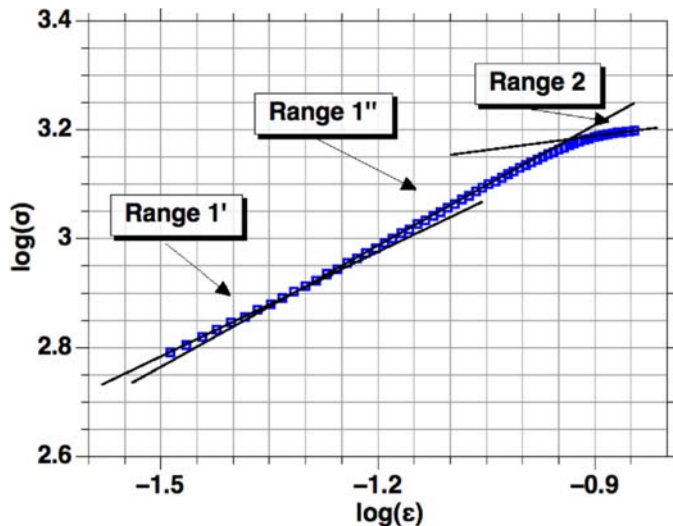
Fig. 6. Example of the occurrence of hardening ranges with additional Range 1' marked on the $\log(\sigma) - \log(\varepsilon)$, applies to samples S5-1, S7-1, S7-2 and S7-3 according with data presented in table 4

TABLE 4

The values of the strength coefficient K_1 and hardening exponent n_1 in Hollomon equation for the AISI 316L/TiB$_2$/2p composites sintered under various conditions of pressure and temperature

Sample	$K_{1'}$	$n_{1'}$	$K_{1''}$	$n_{1''}$	K_2	n_2
S5-1	3.760	0.650	3.850	0.719	3.400	0.232
S5-2	—	—	3.804	0.694	3.165	0.095
S5-3	—	—	3.999	0.768	3.060	0.098
S7-1	3.665	0.577	3.777	0.653	3.295	0.111
S7-2	3.693	0.596	3.826	0.697	3.283	0.115
S7-3	3.716	0.704	3.835	0.787	3.202	0.142

ing temperature, the values of the strength coefficients $K_{1'}$ and $K_{1''}$, also increase, to decrease next in the range of large deformations (K_2). On the other hand, for the hardening exponent n_i, an upward trend was recorded in all the tested ranges. The situation was different in the case of the AISI 316L/TiB$_2$/2p composite produced at a pressure of 5 GPa. In this case, there was no steady upward or downward trend. The values of the strength coefficient and hardening exponent were significantly higher for the sintering temperature of 900°C than for all other variants of the sample treatment, including samples made at a pressure of 7 GPa. However, with the increase of sintering temperature, the changing character of deformation curves caused drop first and increase next in the values of the strength coefficient $K_{1''}$ and hardening exponent $n_{1''}$. In the range of large deformations, the values of the strength coefficient K_2 were decreasing with increasing temperature, while the behavior of parameter n_2 was similar to the composites sintered at a pressure of 7 GPa. It should be noted that for the samples of the S5-2 (5 GPa, 1150°C) and S5-3 (5 GPa, 1300°C) composites, the values of the strength coefficients in the range of large deformations were similar to the values recorded for pure AISI 316L steel, while in other cases, these values were much higher [43,48].

3.3. Discussion of results

Using the results obtained, an attempt was made to explain the source of so significant differences not only in the hardness values, but also in the values of the stress of plastic flow and in the nature of changes in the tested composite hardening range (the values of the strength coefficient and hardening exponent according to Hollomon equation).

Several factors that might affect the examined properties have been taken into account, including the impact of porosity, microstructure and phase transformations on the investigated mechanical properties.

First of all, possible effect of porosity on the obtained results was excluded [49-51]. As stated in Section Physical properties, for all tested samples, the density of the sintered AISI 316L/TiB2/2p composite was the same and related density is 99%. Thus porosity could not be the source of differences in hardness or mechanical characteristics of the deformation.

To describe the ranges of hardening, the literature uses numerous empirical relationships, where one of the most frequently used is the Ludwigson relationship [34,39,46,47]. This relationship was used for the analysis and description of the test composite hardening curves. The analysis of the hardening behavior showed the existence of two different types of curves, both depending on the manufacturing process, as shown in Figure 5.

With the change of sintering parameters changes the size of individual ranges. In accordance with Ludwigson equation (2), the first range of hardening is significantly reduced for all AISI 316L/TiB$_2$/2p composites produced at a pressure of 7 GPa and for the composite sintered at 900°C and 5 GPa. In most cases, the existence of small but interesting, additional range was disclosed in the area of small deformations as shown in Figure 6.

Following the preliminary analysis of the hardening ranges, an attempt was made to describe them with Ludwigson equation. However, this has proved to be possible only in the two selected cases. A correct fit of the experimental and theoretical curves was obtained for two composites only, i.e. (S5-2 and S5-3), sintered at a pressure of 5GPa and at temperatures of 1150°C and 1300°C. In other cases, although the values of strength coefficients K_1 and K_2 and hardening exponents n_1 and n_2 were derived from Ludwigson equation, they did not give a satisfactory fit for the experimental and theoretical data. For this reason, the idea to use Ludwigson equation was given up, and for the description of hardening ranges Hollomon relationship [35,39,46,47] has been used. The obtained values of coefficients K_1 and n_1 for different ranges of hardening are compared in Table 4.

It was assumed that the values of coefficients with index 1' will correspond to the additional range in the area of small deformations, 1'' to further part of the range of small deformations, and 2 to the range of large deformations.

The obtained results clearly demonstrate that for the composite produced at a pressure of 7 GPa, regardless of the examined range (the range of small deformations), with increas-

The next stage of the research included analysis of the composite microstructure. Since mechanical properties of the material are reflected in its microstructure, the occurrence of significant microstructural differences in the test samples was expected. Several factors such as grain size and distribution of the reinforcing phase [23,45,48] were taken into account as possible causes of so large differences in the mechanical properties of two samples. To clarify the doubts, microstructure of all the tested samples was examined by SEM and the results are shown in Figure 7.

Considering the fact that in all the examined cases no major differences were traced in the composite microstructure, Figure 7 shows only the example of microstructure images obtained for the two extreme cases. In all samples, the grain size was observed to be at a similar level (equivalent diameter 24 ± 2 μm), and the same distribution of the TiB$_2$ reinforcing particles has occurred along the alloy matrix boundaries.

The fact that the observed differences were not in the least degree reflected in the microstructure has motivated further studies. So, relying on reports in the literature about the possibility of occurrence of phase transformations in the AISI 316L alloy [52-54], and taking into account significant changes in the equilibrium system at high pressure, X-ray phase analysis was carried out for studied composites. Significant differences

were expected to occur in the phase composition, which might explain the observed changes in mechanical properties. For this purpose, studies were conducted on all prepared samples. Figure 8 shows as an example two diffraction patterns illustrating the phase composition of the composite after sintering. In all the examined cases, also the phase composition has proved to be almost identical.

The analysis of the X-ray diffraction patterns shown in Figure 8 has revealed in the S5-1 composite sintered at 900°C the content of austenite and α phase at a level of 65.5% and 34.5%, respectively. In the S5-3 composite sintered at 1300°C the content of austenite and α phase was at a level of 66.4% and 33.6%, respectively. In other cases, the obtained results were in the same range of values, and differences between them did not exceed 1%. Taking into account the fact that the obtained results demonstrate the lack of differences in the density of the manufactured composites and the lack of any more significant differences in the microstructure or phase composition, it is clear that the adopted research methods are not sensitive enough to allow identification of a mechanism responsible for the observed changes in mechanical properties.

In the present state of studies, a hypothesis can be put forward that the observed changes, both qualitative and quantita-
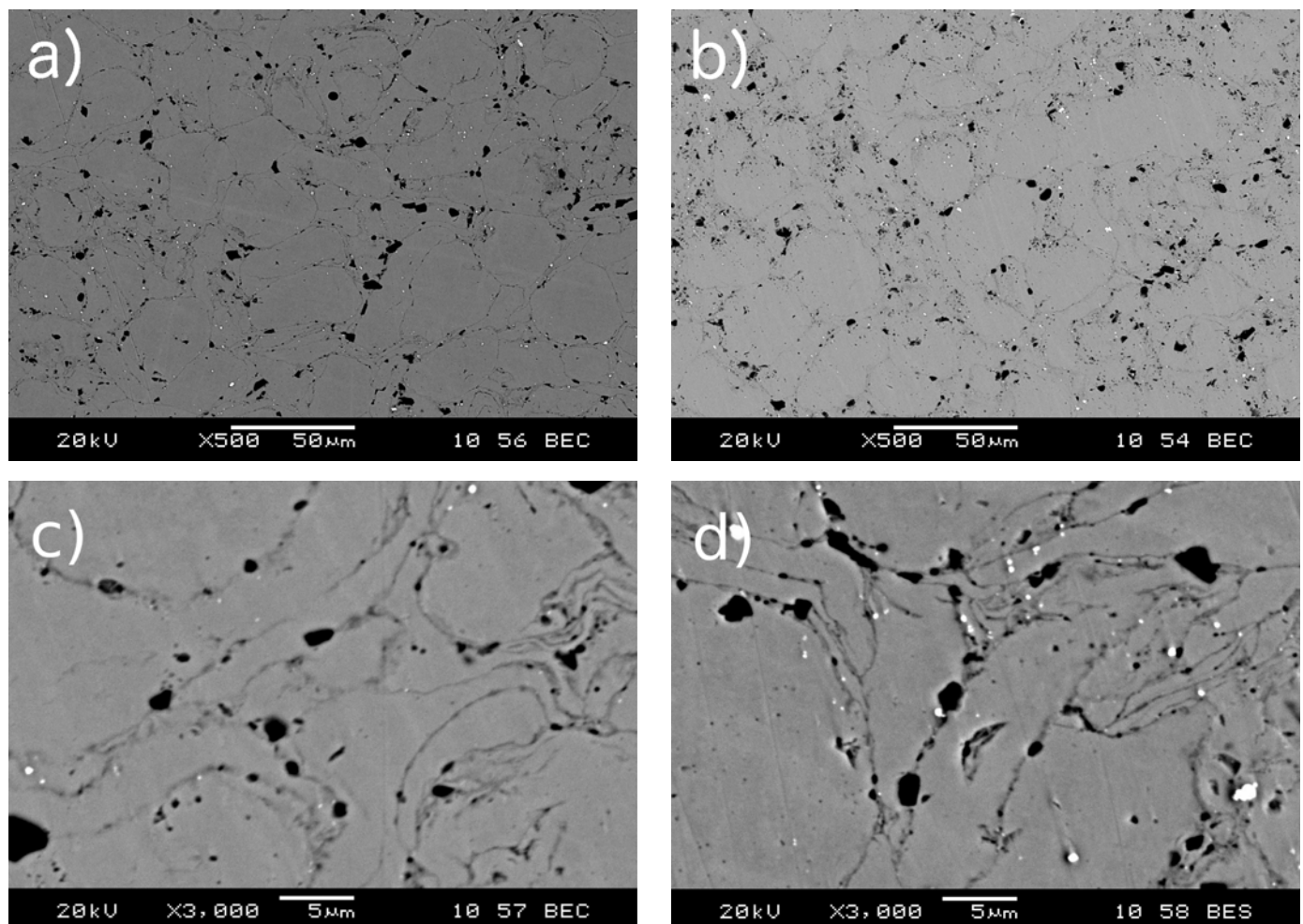

Fig. 7. Examples of microstructure images of the AISI 316L/TiB$_2$/2p composites sintered by the HP-HT method: a) $T = 900$°C, $P = 5$ GPa, mag. 500×; b) $T = 1300$°C, $P = 5$ GPa, mag. 500×, c) $T = 900$°C, $P = 5$ GPa, mag. 3000×; d) $T = 1300$°C, $P = 5$ GPa, mag. 3000×
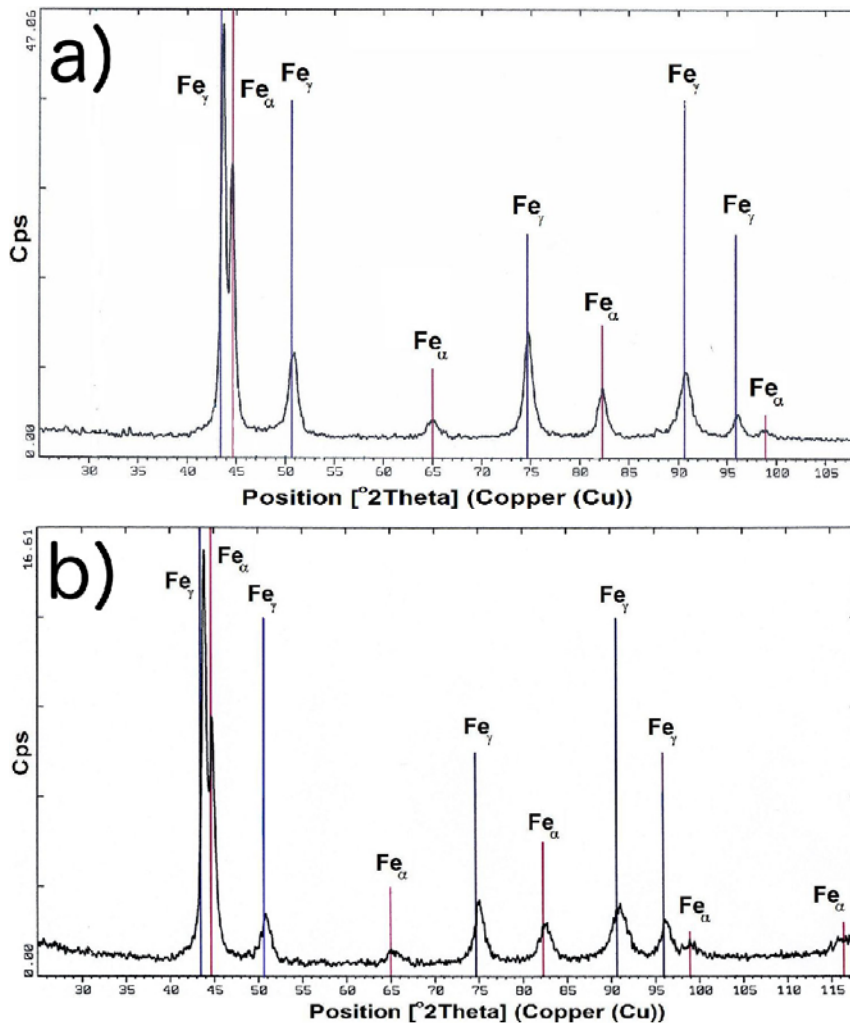
Fig. 8. Examples of analysis of the phase composition of the manufactured composites: a) $T = 900°C$, $P = 5$ GPa; b) $T = 1300°C$, $P = 5$ GPa

tive, in the ranges of hardening and in the values of the stress of plastic flow and hardness of the tested composites may be due to subtle changes in the dislocation structure. These changes are probably the result of a significant and still not fully investigated effect of high pressure and temperature on processes that may occur during sintering. Moreover, the conditions changing at the end of the sintering process, including the variable cooling rate correlated with pressure, may also induce the presence of high internal stresses. Confirmation of this hypothesis requires, however, further more detailed studies using transmission electron microscopy.

4. Conclusions

The obtained results showed significant differences in selected mechanical properties of composites manufactured under varying conditions of pressure and temperature. The exact cause of these differences was not established. The study has proved that:

- Changes in process temperature affect in a significant way the values of hardness and stress of plastic flow. The magni-

tude of this impact is similar for both examined parameters. The maximum differences between the samples were found in the composite produced at a pressure of 5 GPa and temperatures of 900°C and 1300°C. The observed differences in hardness were at a level of about 40%. On the other hand, the recorded maximum increase in the value of the stress of flow was at a level of about 40% too.

- The effect of sintering pressure was increasing with the process temperature increase. For the temperature of 900°C and pressure of 5 GPa and 7 GPa, the observed differences in the examined compressive strength were at a level of 1-2%, but for the temperature of 1300°C they went up to 20%.

- The adopted parameters of the sintering process had significant influence on the value and the hardening ranges, making impossible the use of the popular Ludwigson model to describe the course of hardening.

- There were not visible changes in the density, phase composition, microstructure, distribution of the reinforcing phase, or in the matrix. Therefore the occurrence of very large differences in the dislocation structure of the investigated composites is to be expected.

REFERENCES

[1] B. Basu, G.B. Raju, A.K. Suri, Inter. Mater. Rev. **51** (6), 352-374 (2013).

[2] V.I. Matkovich, Boron and Refractory Borides, Springer Science & Business Media, Berlin, Heidelberg (2012).

[3] R. Koonigshofer, S. Fuurnsinn, P. Steinkellner, W. Lengauer, R. Haas, K. Rabitsch, M. Scheerer, Inter. J. Ref. Met. Hard Mater. **23** (4-6), 350-357 (2005).

[4] N.R. Baddoo, J. Constr. Steel Res. **64** (11), 1199-1206 (2008).

[5] P. Marshall, Austenitic Stainless Steels, Microstructure and mechanical properties, Springer Science & Business Media (1984).

[6] A. Fedrizzi, M. Pellizzari, M. Zadra, E. Marin, Microstructural study and densification analysis of hot work tool steel matrix composites reinforced with TiB_2 particles, Mater. Char. **86**, 69-79 (2013).

[7] E. Olejnik, L. Szymanski, P. Kurtyka, T. Tokarski, B. Grabowska, P. Czapla, Archives of Foundry Engineering **16** (2), 89-94 (2016).

[8] B. Li, Y. Liu, J. Li, H. Cao, L. He, J. Mater. Process Tech. **210** (1), 91-95 (2010).

[9] I. Sulima, R. Kowalik, Mater. Sci. Eng. A **639**, 671-680 (2015).

[10] I. Sulima, L. Jaworska, P. Figiel, Arch. Metall. Mater. **59** (1), 205-209 (2014).

[11] I. Sulima, G. Boczkal, Mater. Sci. Eng. **A 644**, 76-78 (2015).

[12] V. Viswanathan, T. Laha, K. Balani, A. Agarwal, S. Seal, Mater. Sci. Eng. R-Reports **54** (5-6), 121-285 (2006).

[13] E. Olejnik, G. Sikora, S. Sobula, T. Tokarski, B. Grabowska, Materials Science Forum **782**, 527-532 (2014).

[14] E. Olejnik, L. Szymanski, P. Kurtyka, T. Tokarski, W. Maziarz, B. Grabowska, P. Czapla, Archives of Foundry Engineering **16** (3), 77-82 (2016).

[15] E. Fraś, A. Janas, P. Kurtyka, S. Wierzbinski, Arch. Metall. Mater. **48**, 384-408 (2003).

[16] E. Fras, A. Janas, P. Kurtyka, S. Wierzbinski, Arch. Metall. Mater. **49**, 113-141 (2004).

[17] L. Blaz, M. Sugamata, J. Kaneko, J. Sobota, G. Wloch, W. Bochniak, A. Kula, J. Mater. Proc. Tech. **209** (9), 4329-4336 (2009).

[18] K. Bryla, J. Dutkiewicz, L. Litynska-Dobrzynska, L.L. Rokhlin, P. Kurtyka, Arch. Metall. Mater. **57** (3), 711-717 (2012).

[19] B. Mani, M.H. Paydar, J. Alloys Comp. **492** (1-2), 116-121 (2010).

[20] K. Bryla, J. Dutkiewicz, L.L. Rokhlin, L. Litynska-Dobrzynska, K. Mroczka, P. Kurtyka, Arch. Metall. Mater. **58** (2), 481-487 (2013).

[21] R.S. Mishra, Z.Y. Ma, Mater. Sci. Eng. R-Reports **50** (1-2), 1-78 (2005).

[22] G.J. Fernandez, L.E. Murr, Mater. Charact. **52** (1) 65-75 (2004).

[23] P. Kurtyka, N. Rylko, T. Tokarski, A. Wojcicka, A. Pietras, Comp. Structure **133**, 959-967 (2015).

[24] L.-W. Yin, Z.-D. Zou, M.-S. Li, Y.-X. Liu, Z.-Y. Hao, App. Phys. A **71** (4), 457-459 (2000).

[25] P. Klimczyk, V.S. Urbanovich, Arch. Mater. Sci. Eng. **39** (2), 92-96 (2009).

[26] J. Pantic, V. Urbanovich, V. Poharc-Logar, B. Joki, M. Stojmenovi, A. Kremenovi, B. Matovi, Phys. Chem. Minerals **41** (10), 775-782 (2014).

[27] P. Wyzga, L. Jaworska, M. Bucko, P. Putyra, A. Kalinka, Composites **11** (1), 34-38 (2011).

[28] F. Bundy, Ultra-high pressure apparatus, Physics Reports **167** (3), 133-176 (1988).

[29] M. Eremets, High Pressure Experimental Methods, Oxford Science Publications, Oxford University Press, (1996).

[30] L. Jaworska, Materials Engineering **2**, 72-75 (1999).

[31] T. Pieczonka, J. Kazior, A. Tiziani, A. Molinari, J. Mater. Proc. Techn. **64** (1-3), 327-334 (1997).

[32] G.S. Upadhyaya, S.K. Mukherjee, Mater. Des. **6** (6), 323-327 (1985).

[33] I. Sulima, P. Klimczyk, P. Hyjek, Arch. Mater. Sci. Eng. **39** (2), 103-106 (2009).

[34] D.C. Ludwigson, Metall. Trans. **2** (10), 2825-2828 (1971).

[35] H.J. Hollomon., Tensile deformation, Transactions of the Metallurgical Society of AIME **162**, 268-290 (1945).

[36] D. Lee, Metall. Trans. **1** (6), 1607-1616 (1970).

[37] C. Sellars, W.M. Tegart, Inter. Mater. Rev. **17**, 1-23 (1972).

[38] D.J. Drobnjak, J.G. Parr, Metall. Trans. **1** (4), 759-765 (1970).

[39] M. Selin, Metal. Mater. Trans. A **41** (11), 2805-2815 (2010).

[40] S.S. Wu, S.Y. Chen, D. Gan, Mater. Sci. Eng. A **127** (2), L1-L5 (1990).

[41] J.W. Simmons, Metall. Mater. Trans. A **26** (10), 2579-2595 (1995).

[42] J. Lesage, D. Chicot, O. Bartier, M.A. Zampronio, P.E.V. de Miranda, Mater. Sci. Eng. A **282** (1), 203-212 (2000).

[43] E.I. Samuel, B.K. Choudhary, K. Rao, Scr. Mater. **46** (7), 507-512 (2002).

[44] D.J. Lloyd, Scr. Mater. **48** (4) 341-344 (2003).

[45] B. Inem, Mater. Sci. Eng. A **197** (1), 91-95 (1995).

[46] K.G. Samuel, Journal Phys. D: Applied Physics **39** (1), 203-212 (2005).

[47] S. Hertele, W. De Waele, R. Denys, Int. J. Non-Linear Mech. **46** (3), 519-531 (2011).

[48] B.P. Kashyap, K. Tangri, Acta Metall. Mater. **43** (11), 3971-3981 (1999).

[49] N. Kurgan, Mater. Des. **55**, 235-241 (2014).

[50] B. Verlee, T. Dormal, J. Lecomte-Beckers, Pow. Metall. **55** (4), 260-267 (2012).

[51] M. Dewidar, Inter. J. Mech. Mech. Eng. **12** (1), 10-24 (2012).

[52] A. Szymanska, D. Oleszak, A. Grabias, M. Rosinski, K. Sikorski, J. Kazior, A. Michalski, K.J. Kurzydlowski, Rev. Adv. Mater. Sci. **8** (2), 143-146 (2004).

[53] Z.G. Liu, X.J. Hao, K. Masuyama, K. Tsuchiya, M. Umemoto, S.M. Hao, Scr. Mater. **44** (8-9) 1775-1779 (2001).

[54] M. Umemoto, Z. Liu, Y. Xu, K. Tsuchiya, Metall. Mater. Trans. A **33** (7) 2195-2203 (2002).